AIAA SciTech Forum
7-11 January 2019, San Diego, California
AIAA Scitech 2019 Forum

10.2514/6.2019-0639

Reynolds Number Effect on Lift Characteristics of an Airfoil Translating Across a Non-uniform Approach Flow

B. A. Hamedani,[1] A. M. Naguib[2], M. M. Koochesfahani[3]
Michigan State University, East Lansing, MI-48824

We experimentally investigate the lift characteristics of a NACA-0012 airfoil which translates steadily across a non-uniform approach flow. Measurements are conducted in a wind tunnel at a chord Reynolds number of $75k$ for a range of angles of attack (AoA) for both stationary and translating airfoils at various airfoil cross-stream velocities. The motion of the airfoil across the shear zone produces flow unsteadiness that is characterized by the product of the non-dimensional shear rate K and the ratio of the airfoil to freestream velocity V_r. The lift coefficient of the translating airfoil is compared against that of the stationary airfoil while accounting for the former's motion using the uniform-freestream concepts of *effective* freestream velocity and *effective* AoA. The results show that the lift coefficient of the moving airfoil is higher than that of the stationary airfoil at positive AoA. The largest difference is found near stall, where the airfoil motion leads to early stall and a higher maximum lift coefficient. On the other hand, less discrepancy between the static and the moving airfoils is found at negative AoA. Overall, these results demonstrate that the flow around the moving airfoil at AoA near stall is not quasi-steady for the experimental conditions considered in the present work. This finding also holds for a companion study at a smaller Reynolds number of $10k$.

I. Nomenclature

AoA	=	Angle of attack
AR	=	Aspect ratio
b	=	Airfoil span
C_L	=	Lift coefficient = $F_L/(q \times b \times c)$
c	=	Chord length
F_D	=	Drag force in the Galilean frame of reference (see Eq. 3)
F'_D	=	Drag force in the laboratory frame of reference
F_L	=	Lift force in the Galilean frame of reference (see Eq. 3)
F'_L	=	Lift force in the laboratory frame of reference
f_n	=	Natural frequency of the test model
K	=	Non-dimensional shear rate = $(dU_\infty/dy) \times (c/U_o)$
q	=	Dynamic pressure based on an approach-stream velocity scale
Re_c	=	Chord-based Reynolds number
St	=	Strouhal number of airfoil oscillation
U_0	=	Approach-stream velocity at the cross-stream coordinate of the ¼-chord point of the airfoil
U_1	=	Uniform free stream velocity at the high speed side
U_2	=	Uniform free stream velocity at the low speed side
U_c	=	Velocity at the center of shear zone = $(U_1 + U_2)/2$
U_∞	=	Free stream velocity

[1] Graduate student, Mechanical Engineering Department, 1449 Engineering Research Ct. C130, junior AIAA member.
[2] Professor, Mechanical Engineering Department, 1449 Engineering Research Ct. C128, AIAA associate fellow.
[3] Professor, Mechanical Engineering Department, 1449 Engineering Research Ct. A131, AIAA associate fellow.

$U_{\infty,eff}$ = Effective freestream velocity (freestream velocity in a Galilean frame of reference) for the case of the moving airfoil (see Eq. 1)
V_a = Airfoil cross-stream velocity
V_r = Airfoil cross-stream velocity ratio = V_a/U_o
x = Streamwise coordinate
y = Cross-stream coordinate
y_a = Cross-stream coordinate of the ¼-chord point of airfoil
α_{geo} = Geometric angle of attack
α_{eff} = Effective angle of attack for the case of the moving airfoil (see Eq. 2)
Δ = Airfoil free-tip deflection amplitude
δ = Shear-zone thickness
ν = Kinematic viscosity of the fluid

II. Introduction

The focus of traditional aerodynamics research has been mainly on uniform approach flow, while less attention has been paid to non-uniform flows. There are many scenarios in which a uniform approach flow is not a realistic assumption for an airfoil in flight. The specific scenario involving an airplane landing in the presence of wind shear motivates the present investigation. This situation involves the added complexities of both the presence of shear in the freestream, as well as the motion of the wing across the shear zone. The basic aerodynamics of wings/airfoils under such circumstances remain largely unexplored.

Of the few studies conducted to investigate the effect of shear flow on an airfoil, none examines airfoils translating across the shear zone, with most focusing on stationary airfoils. This includes the inviscid theory of Tsien [1], the theoretical and experimental work of Ludwig and Erickson [2], the experiments of Payne and Nelson [3], and more recently the computational study of Hammer *et al.* [4]. Additionally, the investigations by Yu *et al.* [5], and Hammer *et al.* [6] consider periodically oscillating airfoils.

In light of the above, the current work is initiated to experimentally study the fundamental aerodynamic characteristics of an airfoil translating across a shear flow. To simplify the problem, the study only considers an airfoil translating with constant velocity V_a across the shear zone. The flow configuration is depicted schematically in Fig. 1, along with the associated coordinate system, and relevant nomenclature. A velocity scale U_o for the approach stream is *defined* at the cross-stream coordinate of the ¼-chord point of the airfoil y_a; i.e. $U_o = U_\infty(y_a)$. The corresponding relevant non-dimensional parameters are the chord Reynolds number $Re_c = U_o c/\nu$ (c representing the airfoil's chord length), the non-dimensional shear rate $K = (dU_\infty/dy)(c/U_o)$, and the velocity ratio $V_r = V_a/U_o$. As a result of the airfoil motion across the shear zone, the *local* U_o, and therefore the aforementioned non-dimensional parameters, vary with the airfoil position and time. This makes the problem unsteady in general.

The primary objective of the present study is to report on measurements of the lift coefficient (C_L) variation with angle of attack (AoA) for an airfoil traversing a shear zone at $Re_c \approx 75k$ (based on the velocity U_c at the center of the shear zone). A complimentary investigation in a water tunnel [7] involves similar type of measurements at a lower Reynolds number, $Re_c = 10k$. The water-tunnel work will ultimately capitalize on the high-spatial-resolution capability of single-component molecular tagging velocimetry to capture the boundary layer evolution on the suction surface of the airfoil. This enables connecting the measured force behavior with the flow physics. The present paper facilitates examination of whether the force characteristics observed at low Re_c remain unchanged at higher Reynolds numbers using wind tunnel experiments.

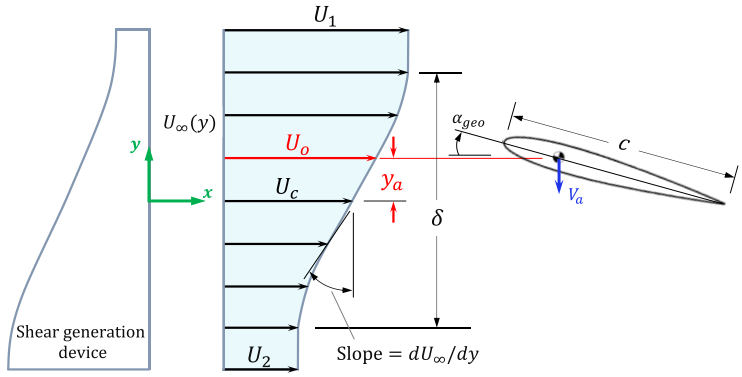

Figure 1. Schematic of the flow configuration depicting the non-uniform freestream velocity $U_\infty(y)$ and the airfoil translating steadily with velocity V_a across the shear zone at a geometrical angle of attack α_{geo}. The coordinate-system's origin is located at the center of shear, where U_∞ equals the average velocity of the high- and the low-speed uniform streams $U_c = (U_1 + U_2)/2$.

Because the present project is the first to involve force measurements on an airfoil that is traversing across a *relatively large fraction* of the test section's width, a significant objective of this investigation is to examine if the tunnel's sidewalls and the model blockage, coupled with the airfoil motion could lead to force measurement artifacts. To this end, force measurements on static and moving airfoils are compared *when the freestream is uniform.* In the absence of measurement artifacts, the forces acting on a static airfoil, at a given AoA and freestream velocity, should be the same as those acting on a steadily moving airfoil, having the same AoA and freestream velocity in a Galilean transformed (GT) frame of reference (i.e. in a coordinate system that is moving with the airfoil). The AoA and the freestream velocity in the GT frame are usually termed the *effective* AoA and the *effective* freestream velocity of the moving airfoil.

Another objective of this study is to compare static- and moving-airfoil force data when shear is present in the freestream. This objective is motivated by investigating if a GT would also be useful in connecting static- and moving-airfoil forces in a shear zone. Such a connection would be useful in alleviating the need to conduct moving-airfoil experiments and computations to characterize the load on an airfoil traversing across a shear zone.

III. Experimental Setup and Procedure

Experiments are conducted in an open-circuit wind tunnel, with a 61 cm-high × 61 cm-wide × 183 cm-long test section, at the Flow Physics and Control Laboratory at Michigan State University. The test section is divided into an upper and a lower part using a false wooden ceiling, as sketched in Fig. 2. The upper part accommodates various instruments, while the lower part is used for measurements. An Instrument Plate is inserted in the false ceiling to mount several of the main components of the setup. This includes a Parker T2D Triology linear servo motor/positioner to translate the airfoil with a prescribed motion profile across the test section. The positioner is capable of traversing over a distance of 36.6 cm at speeds up to 2.5 m/s. The resolution and the repeatability of positioning are 1 and 2 μm respectively, while the accuracy is better than 0.1 mm, per manufacturer's specifications.

A 55 mm-wide rectangular slot in the instrument plate allows connection between the carriage of the servo motor and an instrumented NACA-0012 airfoil below the false ceiling. This slot is capped with a sealed rectangular box to prevent air leakage between the upper and the lower sides of the false ceiling. The airfoil, which has a chord length c = 12 cm and an aspect ratio AR=1.8, is attached to the servo motor through a rectangular shaft, two adapters, and a load cell (ATI-Mini 40); all mounted co-axially, as demonstrated in Fig. 2. The axis of the load cell coincides with the ¼-chord point of the airfoil, which is located 130 cm downstream of a shear generation device, placed at the entrance of the test section. The load cell is capable of measuring all six components of load. Only force measurements in x and y directions; i.e. streamwise and cross-stream directions respectively, are used in the present study. For these two components, the load cell has a range of 20 N and a resolution of 0.005N. This corresponds to a force coefficient values of 13.7 and 0.0034 respectively, based on the airfoil planform area and the dynamic pressure at the nominal flow velocity of the measurements.

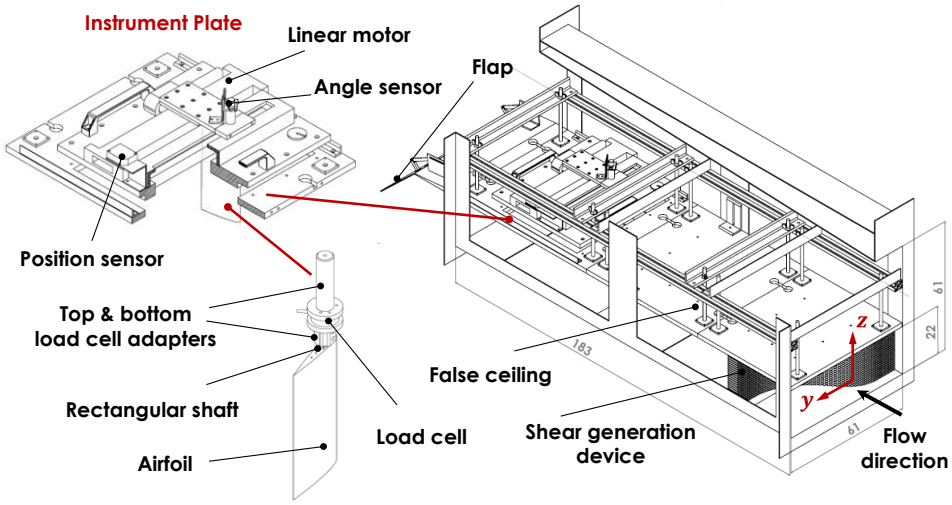

Figure 2. Schematic of the experimental setup. Dimensions are in cm.

Variation in the AoA, and the cross-stream position of the airfoil are measured via a Hall effect angle sensor (Vishay 981 HE, with a range of $0-90°$, and linearity error $\pm 0.5\%$), and a triangulation laser sensor (Baumer OADM 20U2480/S14F, range $100-600mm$, linearity error $\pm 0.05-\pm 2.00\ mm$), respectively. To set the zero AoA, the airfoil is first oriented with the chord parallel to the test section's sidewalls. This setting is refined further using force measurements to find the angle corresponding to the minimum force magnitude (including drag and lift components) in *uniform freestream*. The difference between the geometrically-set and the force-measurement-based zero AoA is typically less than 0.5°. In addition, the small misalignment between the load cell axes and the drag and the lift directions (typically around 1°) at zero AoA is found based on the zero-crossing of the lift component, and accounted for in data conversion.

A flap at the downstream end of the false ceiling is used to position the ceiling's leading-edge separation on the upper (instrumentation) side of the ceiling. This is done in order to avoid flow unsteadiness due to separation on the lower (measurement) side. A variable-length, 3.175 mm-cell-diameter honeycomb structure is placed at the test section's entrance below the false ceiling to produce prescribed velocity variation across the test section. Although it is desirable to shape the honeycomb to generate the simplest form of shear; i.e. uniform-shear, or linear velocity profile, an already available honeycomb device is employed for the present measurements. This honeycomb was originally designed, following the work of Kotansky [8] and Safaripour *et al.* [9] to produce a hyperbolic-tangent velocity profile in a water tunnel at a much lower freestream velocity. When placed in the wind tunnel, the resulting freestream mean-velocity profile is shown in Fig. 3 (a). The velocity measurements are done using a pitot tube, connected to a 124.7 Pa-range Setra pressure transducer (model 239), 115 cm downstream of the exit of the shear generator with the airfoil removed. When the airfoil is placed in the test section at zero AoA, its leading edge is approximately one chord length downstream of where the velocity profile is measured.

The mean-velocity profile in Fig. 3 depicts the presence of a two-stream shear layer with a shear-layer thickness to airfoil chord ratio of $\delta/c = 0.51$. The edges of the shear zone δ are identified at the locations where the mean velocity gradient in the shear zone drops to 5% of its highest magnitude (approximately at the center of shear) on both the high- and the low-speed sides. The high- and low-speed freestream velocities are determined to be $U_1 = 11.9\ m/s$ and $U_2 = 7.4\ m/s$, respectively, from averaging the approximately-flat portions at the two ends of the profile. The velocity at the center of the shear layer is $U_c = 9.65\ m/s$, based on the average of U_1 and U_2. In Fig. 3, the profile exhibits some undesirable imperfections in the form of an undershoot at the low-speed shear-layer edge, and spatial non-uniformities in the freestream (corresponding to spatial *rms* variation of less than 0.7 % on the high-speed side). Aside from this, smooth velocity variation is seen within the shear zone, corresponding to $K = 1.37$ at the center of shear. This means that the shear rate would cause a velocity change of 37% of U_o over a cross-stream distance equal to the airfoil's chord.

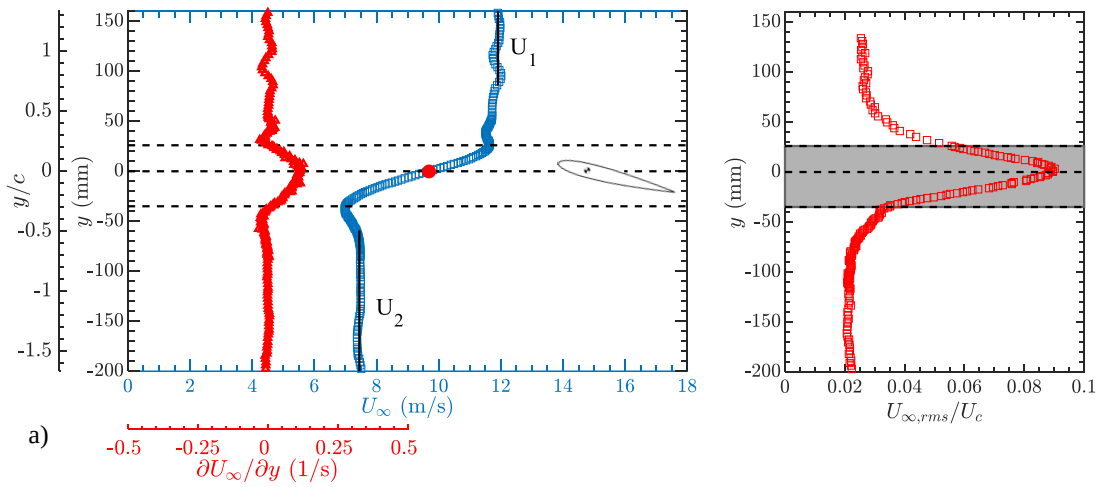

Figure 3. (a) Cross-stream profiles of the mean velocity (blue line) and the mean-velocity gradient, and (b) the *rms* velocity fluctuation of the freestream at 115 cm downstream of the shear generation device. The data are measured without the presence of the airfoil, at a location that is approximately one chord upstream of the airfoil's leading edge when the airfoil is placed at zero AoA. In the left plot, the horizontal broken lines mark the center and edges of the shear layer. The red circle at the shear center shows the cross-stream airfoil position at which lift measurements are conducted. The airfoil is shown to scale at $\alpha_{geo} = +14°$ for reference.

The shear approach stream established in the present work is inherently unsteady. This may be seen from Fig. 3 (b), where the profile of the root-mean-square (*rms*) velocity fluctuation is displayed across the shear zone. The profile is obtained employing a single hot wire operated in the constant temperature mode using Dantec MiniCTA anemometer. The hot wire is calibrated against a pitot tube in the high-speed stream before and after measurements. Agreement between the two calibrations is typically within 1%. As seen from Fig. 3, the fluctuations in the streamwise freestream velocity $U_{\infty,rms}$ exhibits non-uniform variation with a maximum of approximately 9% U_c at the shear center. This behavior is qualitatively similar to that of a traditional two-stream shear layer.

The airfoil is tested in both uniform and shear flow, with each experimental set consisting of both stationary- and moving-airfoil experiments. For the stationary-airfoil measurements, the lift coefficient is measured at the center of the tunnel (also the center of shear for the case of shear flow) at different geometrical angles of attack α_{geo}. The measurement location is identified in Fig. 3 with a red circle. In the moving-airfoil experiments, the airfoil accelerates from one side of the tunnel (the high-speed freestream U_1 for the shear flow) to a steady translation velocity across the shear zone, before decelerating to a stop at the other side (the low-speed freestream U_2 for the shear flow). The whole motion is repeated 50 times for several AoAs in the range $-16° \leq \alpha_{geo} \leq +14°$. These experiments are conducted at three different airfoil velocities $V_a = 100, 225,$ and $450\ mm/s$, corresponding to velocity ratio $V_r = V_a/U_o = 1.1\%, 2.3\%$ and 4.6%, respectively, at the shear center.

A sample motion trajectory of the airfoil for $V_r = 4.6\%$ is shown in Fig. 4. The plot depicts the time history of the airfoil's position, velocity, and acceleration during the motion stroke. As indicated on the figure, the airfoil translates steadily between the cross-stream coordinates -100 mm to 100 mm, which fully encompass the shear zone (as seen from comparison with the shear-layer edges in Fig. 3). This demonstrates that the airfoil reaches and maintains a steady translation velocity throughout the shear zone.

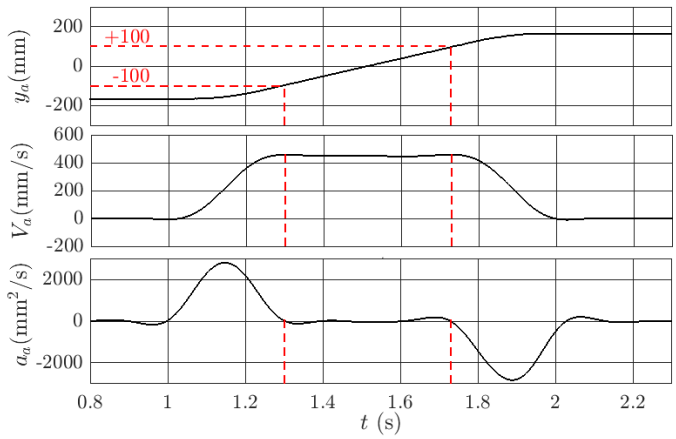

Figure 4. Motion trajectory of the airfoil across the tunnel: cross-stream position (top), velocity (middle), and acceleration (bottom). The duration of constant airfoil velocity corresponds to the period of zero acceleration (defined within a threshold of ±2.5 mm/s^2, or ±0.1% of peak acceleration) after the initial acceleration and before the final deceleration (as delineated with red broken lines). The corresponding cross-stream positions of the airfoil are -100 mm and 100 mm, respectively, as shown on the top plot.

For the shear approach stream, all measurements of the force acting on the airfoil are done at the center of the shear zone. The corresponding Reynolds number is $Re_c = U_o c/\nu = U_c c/\nu \approx 75k$. This value is maintained the same for measurements in the uniform freestream. The freestream velocity is set and monitored using a pitot tube connected to the Setra pressure sensor discussed previously. For the shear flow, the pitot tube is used to monitor the high-speed-stream velocity.

IV. Data Acquisition and Analysis

Six voltage signals from the load cell, the wind tunnel freestream velocity (pressure transducer voltage), and the airfoil ¼-chord-point cross-stream position (triangulation sensor voltage) are recorded at 2000 Hz using a National Instruments DAQ system (NI 6034E with 16 bit resolution and maximum sampling rate of 200 kS/s) with eight differential input channels. The load cell exhibits a slight slow drift over time, the effect of which is taken into account by conducting zero-load measurements before and after the experiments. For the static airfoil, data are recorded for 60 s, corresponding to 4825 c/U_o at the center of shear and in uniform flow.

For the moving airfoil experiments, data are acquired during 50 strokes of motion and are phase-averaged relative to the start of the motion. With the same data sampling rate as the stationary airfoil, the airfoil translates a distance of $0.0019c$ between successive data points at the largest airfoil velocity. Since all measurements of interest are carried out during the steady-translation phase, the results are unaffected by inertia forces due to linear acceleration of the model. However, the initial "sudden" acceleration of the cantilever-supported model causes slowly-damped mechanical structural oscillation at the natural frequency of the model ($f_n = 36\ Hz$) that persist into the steady motion phase for around 1 second. Using a strobe light to image the airfoil during motion, it is found that the largest deflection at the free tip of the airfoil due to the oscillation is less than 0.5 mm ($0.4\%c$). The corresponding Strouhal number of the oscillation ($St = f_n \Delta / U_o$; where Δ is the deflection amplitude at the airfoil free tip) is less than 0.0019, which is expected to be too small to have a significant influence on the aerodynamic force acting on the airfoil. This conclusion is supported by the agreement between the lift coefficient of the moving and the static airfoil in uniform flow (see section V-A and Fig. 5).

Based on the above, the natural oscillations of the model during motion are not expected to alter the load acting on the airfoil. However, the oscillations do result in an oscillatory inertia force signature that must be removed from the measured force data. For this purpose, all the measured force components are filtered with a fourth-order Butterworth digital filter with a cutoff frequency of 8Hz. This frequency is selected to cancel the force signature at 36 Hz while leaving intact the force variation due to translation of the airfoil across the shear zone. It should be noted that other high-frequency aerodynamic forces, such as that associated with vortex shedding in the wake of the airfoil are not captured in the present measurements. Since the start of the motion of the airfoil is not phase-locked to the vortex shedding cycle, it is expected that the phase-averaging process would remove the corresponding unsteady force signature.

Measurements in uniform flow are conducted as an *a priori* validation of the current experimental procedure. This procedure is different from traditional aerodynamic load measurements, where the airfoil is fixed at the center of the test section, or undergoes oscillatory motion over an amplitude that is much smaller than the width of the test section. The present measurements are conducted during movement of the airfoil over more than 50% of the test section's width. Thus, it is necessary to check that such a motion does not introduce significant measurement artifacts due to model blockage and facility confinement effects. To this end, the lift force measured on the static airfoil is compared to its counterpart on the moving airfoil at the instant when the latter is located at the same cross-stream coordinate as the former. It is well known that the force acting on the airfoil in the two cases must be the same under a Galilean transformation of the moving airfoil. In the GT frame, the effective freestream velocity and angle of attack α_{eff} are connected to the laboratory-frame freestream velocity U_∞ and geometrical AoA as follows:

$$U_{\infty,eff} = \sqrt{U_\infty^2 + V_a^2} = U_\infty\sqrt{1 + V_r^2}, \tag{1}$$

$$\alpha_{eff} = \alpha_{geo} + \tan^{-1}\frac{V_a}{U_\infty} = \alpha_{geo} + \tan^{-1} V_r = \alpha_{geo} + \alpha_{V_r}. \tag{2}$$

Accordingly, the drag and the lift force in the Galilean frame (F_D and F_L, respectively) are computed from the forces in laboratory frame (F'_D and F'_L) via rotation of the laboratory frame through angle α_{V_r}, as given by the following transformation:

$$\begin{bmatrix} F_L \\ F_D \end{bmatrix} = \begin{bmatrix} Cos\ \alpha_{V_r} & Sin\ \alpha_{V_r} \\ -Sin\ \alpha_{V_r} & Cos\ \alpha_{V_r} \end{bmatrix} \begin{bmatrix} F'_L \\ F'_D \end{bmatrix}. \tag{3}$$

The ability to connect the static and the moving airfoil forces via GT becomes more complex in the presence of shear. In this case, the use of Eqs. 1 and 2 entails replacement of U_∞ with the shear-stream's velocity scale U_o. However, since the choice of the ¼-chord reference point and the corresponding velocity scale is arbitrary, it is evident that the effective approach stream velocity and AoA are not unique. This difficulty arises from the cross-stream variation of the freestream velocity, making it impossible to decide which approach stream velocity should be used to compute the effective velocity and α_{eff}. Notwithstanding this difficulty, in the present work, U_o at ¼ -chord point is utilized to transform force measurements from the laboratory to GT frame. This enables examination of whether such a transformation can be useful in approximating the moving-airfoil forces from their static-airfoil counterpart. Physically, it is reasonable to expect that such an approximation would be good in the limit of weak shear; i.e. $K \to 0$, or "quasi-uniform flow". Moreover, since U_o varies with the airfoil position in the shear zone, and hence with time for the moving airfoil, the flow is unsteady in the GT frame of reference. Therefore, equality of forces for the static and GT-transformed-moving airfoils would require the motion to also be quasi-steady; i.e. for the rate of change of U_o with time to be sufficiently small for the flow around the airfoil to adapt to local conditions. Non-dimensionally, this rate of change may be expressed as follows:

$$\frac{dU_o}{dt}\frac{c}{U_o^2} = \frac{dU_\infty}{dy}V_a\frac{c}{U_o^2} = KV_r. \tag{4}$$

Eq. 4 shows that quasi-steadiness is expected in the limit $KV_r \to 0$.

V. Results and Discussion

A. Uniform Flow Results

Fig. 5 provides a comparison of the variation of the lift coefficient (C_L) with AoA for the stationary and the moving airfoils at three locations across the test section for uniform approach flow at $Re \approx 75k$. For the moving airfoil, the angle of attack is presented in the Galilean frame (Eq. 2); i.e. α_{eff}, and the dynamic pressure used to calculate C_L is based on $U_{\infty,eff}$ (Eq. 1). The uncertainty in the phase-averaged lift is estimated from the *standard deviation* of the cycle-to-cycle variation in C_L when the airfoil is located at the position of the comparison. The lift coefficient uncertainty is smaller than the symbol size, while the AoA uncertainty is approximately the same size as the symbols. The excellent agreement between the static- and the moving-airfoil's $C_L - \alpha$ characteristics, including near stall, demonstrates the viability of the moving-airfoil lift measurements over the domain of the comparison (within 25% of the test section width, or $\pm 75\ mm$ (corresponding to $y_a/c = \pm 0.625$) from the shear center when shear is present in the freestream). Comparison with Fig. 3 shows that this domain encompasses the region of interest for measurements in shear approach stream. The results in Fig. 5 provide the required validation of the present experimental approach prior to the shear-flow measurements.

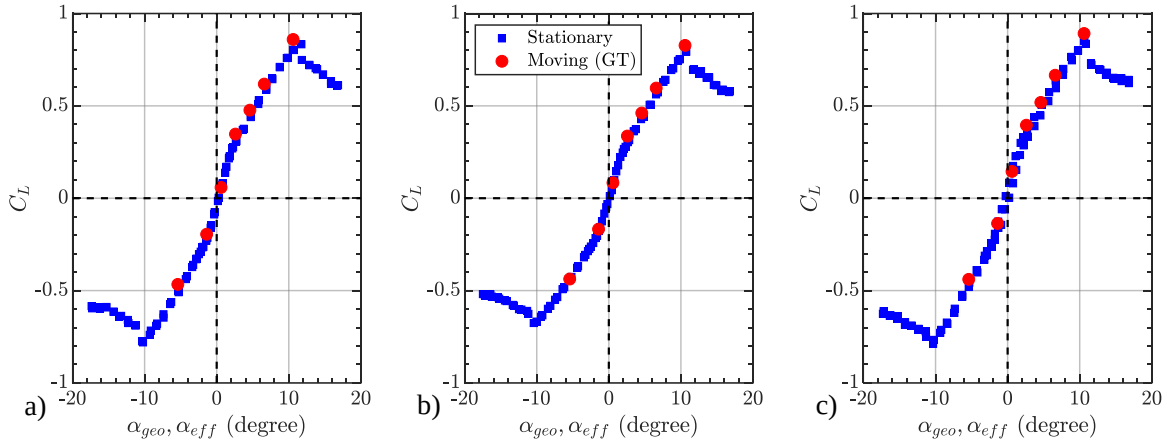

Figure 5. The moving airfoil's phase-averaged-C_L variation with AoA in uniform flow, compared with the time-averaged lift coefficient for the stationary airfoil at three different locations across the test section: a) $y_a/c = -0.625$, b) $y_a = 0$, c) $y_a/c = +0.625$. α_{eff} is defined based on Eq. 2. GT indicates results are presented in a Galilean-transformed frame of reference.

B. Shear Flow Results

For the freestream with shear, the airfoil is translated from the high- to the low-speed side, following the motion profile depicted in Fig. 4. Fig. 6 (a) displays a sample time history of the phase-averaged F_L for $\alpha_{geo} = 10°$ and $V_r = 4.6\%$ (black line). The red lines show F_L data for all 50 strokes used in the phase average. The figure also contains the concurrent airfoil cross-stream position relative to the center of the shear layer. The period corresponding to constant-velocity translation of the airfoil (linear position variation) is indicated in the figure. Outside this period, F_L exhibits a prominent peak and valley associated with the initial acceleration and final deceleration of the airfoil respectively. In the present study, only the period of steady airfoil translation is of interest. Thus, the phase-averaged F_L history during this period is extracted and plotted versus the cross-stream position of the airfoil, as exemplified for three geometrical AoAs in Fig. 6 (b). Within this cross-stream domain, data are extracted at the center of shear (indicated with circles on the plot).

A feature of the force history observed in Fig. 6 (b) is the difference between the lift variation at small and large AoA as the airfoil translates across the shear stream. From a quasi-steady point of view, as the airfoil at a particular α_{geo} moves towards the low-speed side, the effective AoA increases; therefore, a higher lift magnitude is expected. On the other hand, the airfoil's translation is associated with a decrease in freestream velocity (loss of dynamic pressure), which in turn produces a smaller lift force. For the *current airfoil and shear conditions*, at $V_r = 4.6\%$, the effect of force reduction due to dynamic pressure loss seems to outweigh the increase in α_{eff} at large AoA ($\pm 10°$ in Fig. 6 (b)), leading to a drop in the lift magnitude across the shear zone. In contrast, at AoA of $-3°$, α_{eff} switches from a negative to a positive value during translation. This switch is associated with the lift force crossing zero near the shear center. It is emphasized that these interpretations, while consistent with the observations, do not take into account any changes in the lift characteristics of the airfoil across the shear zone and unsteady effects.

Using F_L time histories like those shown in Fig. 6 (b), the value of the lift at the shear center is extracted for several geometrical AoA. The resulting $C_L$versus α_{eff} plot is shown in Fig. 7 for the case of $V_r = 4.6\%$. The figure contains data from several independent experiments to demonstrate the repeatability of the results. The variation in the C_L values from different runs is characterized using the standard deviation, which is combined with a student t-test 5% confidence to estimate the uncertainty in the measurements (depicted on later plots using error bars).

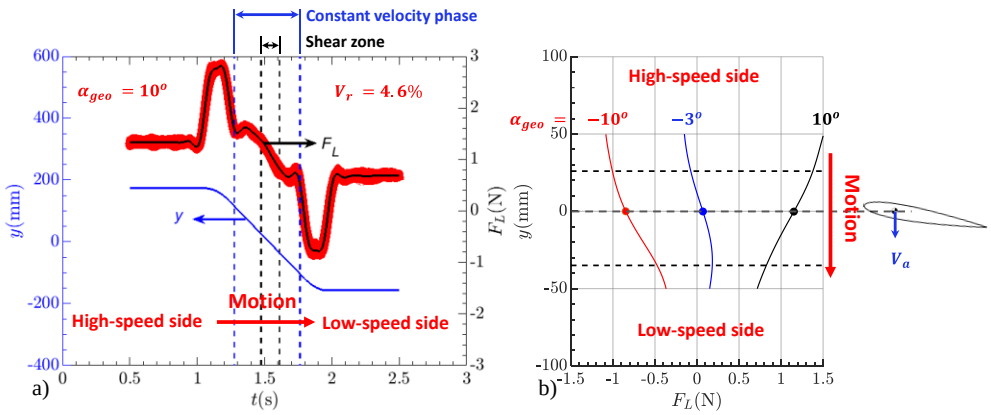

Figure 6. (a) An example of the phase-averaged lift time history for $\alpha_{geo} \approx 10°$ (black line). The red lines represent 50 time histories from the individual airfoil motion strokes used to obtain the phase average. The solid blue line shows the concurrent airfoil position. (b) Example phase-averaged lift variation with cross-stream position of the airfoil for three AoA during the time when the airfoil is translating steadily. The black dashed lines indicate the center and the edges of the shear zone.

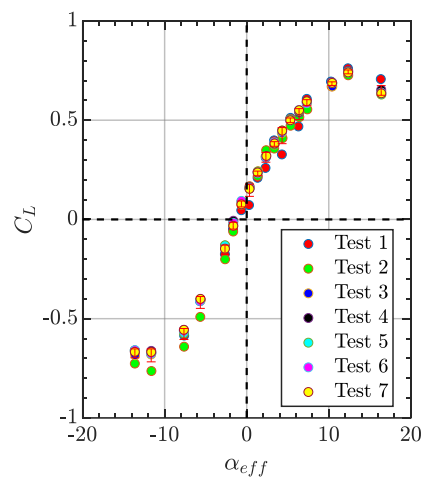

Figure 7. Repeatability of the phase-averaged lift coefficient obtained from different experiments when the airfoil crosses the center of shear ($y_a = 0$). $V_r = 4.6\%$, $K = 1.37$ and $Re_c \approx 75k$.

The results from the different tests in Fig. 7 are averaged and the outcome is shown in Fig. 8. The latter figure also contains static-airfoil data at the same cross-stream position of the moving airfoil ($y_a = 0$) for comparison. One interesting feature seen from comparing this figure to Fig. 5 (b) is the difference of the lift-coefficient characteristics for the stationary airfoil in shear versus uniform flow. Particularly notable is the change in the stall characteristics, where the presence of shear causes the maximum positive lift coefficient to drop by approximately 20%, while the stall angle increases from 10.5° to possibly beyond the range of AoA investigated. Moreover, the stall becomes more gradual in shear, as seen from the broader C_L peak. For a NACA 0018 airfoil at $Re = 150K$, Payne and Nelson [3] also observed freestream shear to produce a delay in the stall angle (by $2° - 3°$). On the other hand, this delay was accompanied by an increase in the maximum C_L, opposite to the present observation. It should be noted, however, that the non-dimensional shear rate K in [3] was approximately an order of magnitude smaller than that in the current study ($K = 0.11$ versus $K = 1.37$, respectively). In addition, those experiments were conducted in a uniform-shear zone that spanned approximately 80% of the test section width and contained a uniform distribution of relatively low-intensity turbulence (0.5%). The latter is distinctly different from the present $U_{\infty,rms}$ profile (Fig. 3).

Another feature of the static-airfoil characteristics in Fig. 8 is that the lift is slightly positive ($C_L = 0.15$) at $\alpha_{geo} = 0^o$. The presence of positive lift at zero AoA (or equivalently a negative zero-lift AoA) in the presence of steady uniform shear in unbounded approach stream was first noted by Tsien [1] in his inviscid solution of the flow

around a Joukowsky airfoil. Though the present results are qualitatively consistent with inviscid theory, the agreement may be serendipitous since the present approach stream is viscous, unsteady and exhibits a non-uniform shear profile.

Comparing the stationary and the moving airfoil results in Fig. 8 shows that the motion of the airfoil changes the lift characteristics in a certain AoA range. The difference is largest in the vicinity of the positive stall angle, where the motion causes the maximum C_L to increase (by approximately 20%) and the stall to occur at an AoA smaller than that of the stationary airfoil (the stall angle for the latter may be larger than the maximum AoA examined here). On the other hand, the static and the moving airfoils seem to have the same lift characteristics at pre-stall negative AoAs.

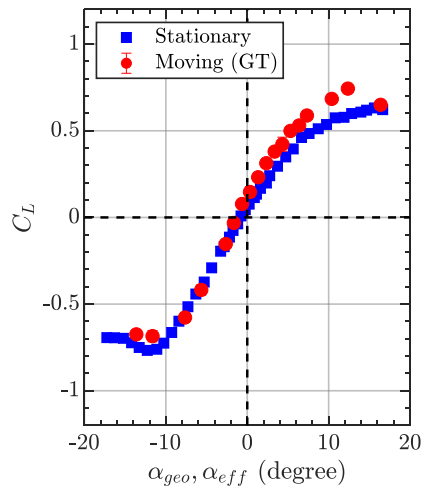

Figure 8. The moving airfoil's phase-averaged-C_L variation with AoA in shear flow, compared with the time-averaged lift coefficient for the stationary airfoil at the center of shear ($y_a = 0$). α_{eff} is defined based on Eq. 2. GT indicates results are presented in a Galilean-transformed frame of reference.

Eq. 4 indicates that the flow unsteadiness is characterized by the non-dimensional parameter KV_r. To examine this further, it is desirable to vary each of K and V_r separately; i.e. one at a time. In the present study, the effect of varying V_r alone is investigated. Future work will target variation of K while maintaining V_r unchanged. Fig. 9 shows the moving-airfoil lift characteristics on the shear layer center for different airfoil velocity ratios. As expected, the discrepancy between the moving and the stationary airfoil results decreases with reducing V_r.

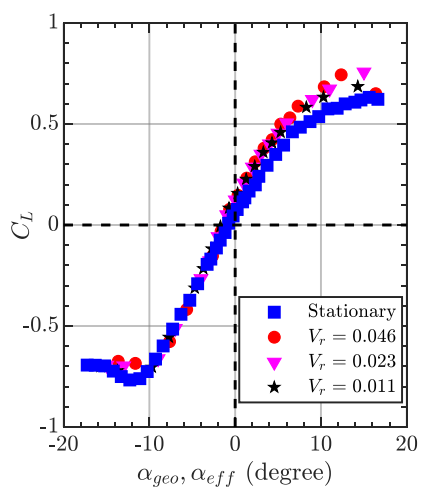

Figure 9. The moving airfoil's phase-averaged-C_L variation with AoA in shear flow, compared with the time-averaged lift coefficient for the stationary airfoil at the center of shear ($y_a = 0$). Different symbols correspond to different values of V_r but the same non-dimensional shear rate ($K = 1.37$). The moving airfoil results are presented in a Galilean frame, moving with the airfoil.

As stated in section II, one of the main objectives of this study is to examine if Reynolds number has an important influence on the lift characteristics of an airfoil moving across a uniform-shear zone. To this end, the present results are compared in Fig. 10 to those obtained by Albrecht $et\ al.$ [7] in a water tunnel at $Re_c = 10k$. In both cases, the static-airfoil results are also shown for reference. For both Reynolds numbers, a qualitatively similar deviation is observed between the static and the moving airfoils at both positive and negative AoAs. Specifically, in both cases a pronounced change in stall characteristics is seen at positive angles. This change leads to stall occurring at a smaller angle of attack and an increase in $C_{L,max}$ when the airfoil is moving.

Notwithstanding the similar qualitative trends, the lower Re_c data exhibit a larger difference between the stationary and the moving airfoil results at positive AoA. At negative AoA, stall characteristics change very little for both cases, with the maximum lift magnitude increasing slightly with airfoil motion for the lower Reynolds number. It should be noted that the comparison between the water and the wind tunnel tests does not take into account factors other than Re_c that are different between the two experiments. This includes the different turbulence characteristics (compare the profile in Fig. 3 to a practically flat u_{rms} distribution of 2-3% intensity in the case of the water tunnel [7]), the shear width ($2c$ for the water tunnel versus $0.51c$ for the wind tunnel), the airfoil aspect ratio ($AR = 5.14$ versus 1.8 in water and air, respectively), and the shear profile details, which is not uniform in the present work.

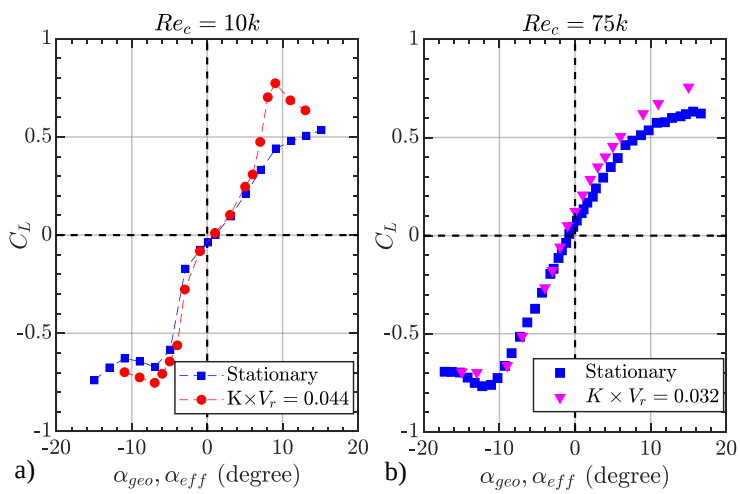

Figure 10. Reynolds number effect on the comparison between the lift coefficients of the stationary and the moving airfoil in a uniform-shear zone: (a) water-tunnel measurements [7] at $Re_c = 10k$, and (b) present data on the tunnel centerline at $Re_c \approx 75k$.

VI. Conclusions

The results presented here demonstrate the viability of a new experimental setup for investigating forces acting on airfoils traversing across a substantial fraction of the test section's width. This demonstration is accomplished by comparing C_L data between stationary and moving airfoil experiments in uniform flow, for a range of AoA and different cross-stream locations. The results yield the same lift characteristics for the stationary and the moving airfoils when accounting for the motion of the airfoil using an *effective* freestream velocity and *effective* angle of attack. This finding is specific to a zone extending 25% of the width in the middle of the test section and for airfoil translation velocities up to approximately 5% of the freestream velocity.

The new experimental setup is utilized to study the lift force acting on an airfoil translating steadily across an approach shear flow. Drawing an analogy with translating airfoils in uniform freestream, the lift coefficient of the moving airfoil in shear flow is defined using an effective freestream velocity, and the results are presented versus an effective AoA. Unlike the case of uniform freestream, the definition of these "effective parameters" is not unique since the approach stream velocity is non-uniform. Nevertheless, this way of framing the results facilitates comparison between the lift coefficient of the moving airfoil with that of its stationary counterpart at the same location within the shear flow. The comparison shows that the lift characteristics of the moving and the stationary airfoils agree over a limited range of AoA. A relatively large deviation between the two cases is found near stall at positive AoA. Specifically, the stall angle decreases and the maximum lift coefficient increases as a result of the airfoil motion. The comparison is carried out where the Reynolds number is approximately 75,000. Overall, the

results suggest that the flow around the airfoil is not quasi-steady (except for a limited range of AoA) for the shear flow and the airfoil parameters considered here.

The motion of the airfoil across the non-uniform approach flow is associated with a change in the local freestream velocity scale U_o. The unsteadiness in U_o is characterized by the non-dimensional parameter KV_r (where K is the non-dimensional shear rate, and V_r is the ratio of the airfoil to approach stream velocity). The impact of V_r is investigated in this study by changing the cross-stream velocity of the airfoil while maintaining the same approach stream conditions. The results depict a monotonically increasing deviation between the static and the moving airfoil lift characteristics with increasing V_r.

The present data are compared with the results from a companion study in a water tunnel [7] at a smaller Reynolds number of $10k$. In both cases, the deviation between the lift characteristics of the static and the moving airfoils exhibit the same qualitative behavior, but the deviation is smaller at the higher Reynolds number. However, the quantitative differences between the water and the air experiments may be caused by factors other than the Reynolds number, which are not matched between the two experiments. These include the airfoil's aspect ratio, the velocity profile across the shear-layer width, the turbulence intensity of the freestream and the values of K and V_r.

Acknowledgments

The authors would like to thank the contribution and technical assistance of Dr. David Olson in conducting these experiments. This project is funded through ONR grant number N00014-16-1-2760. The views and conclusions contained in this document are those of the authors and should not be interpreted as representing the official policies, either expressed or implied, of ONR or the U.S. Government. The U.S. Government is authorized to reproduce and distribute reprints for Government purposes notwithstanding any copyright notation herein.

References

[1] H. S. Tsien, "Symmetrical Joukowsky Airfoils in Shear Flow," *Quarterly of Applied Mathematics*, pp. 130-148, 1943.

[2] G. R. Ludwig J. C. Erickson, "Airfoils in Two-Dimensional Nommiformly Sheared Slipstreams," *J. Aircraft*, vol. 8, no. 11, pp. 874-880, 1971.

[3] F. M. Payne R. C. Nelson, "Aerodynamic Characteristics of an Airfoil in a Nonuniform Wind Profile," *J. Aircraft*, vol. 22, no. 1, pp. 5-10, 1985.

[4] P. R. Hammer, M. R. Visbal, A. M. Naguib, M. M. Koochesfahani , "Lift on a Steady 2-D Symmetric Airfoil in Viscous Uniform Shear Flow," *J. Fluid Mech*, vol. 837, no. doi: 10.1017/jfm.2017.895, 2018.

[5] M. Yu, B. Wang, Z.J. Wang S. Farokhi, "Evolution of Vortex Structures Over Flapping Foils in Shear Flows and Its Impact on Aerodynamic Performance," *J. of Fluids and Structures*, vol. 76, pp. 116-134, 2018.

[6] P. R. Hammer, D. A. Olson, M. R. Visbal, A. M. Naguib M. M. Koochesfahani, "An Investigation of the Aerodynamics of a Harmonically-Pitching Airfoil in Uniform-Shear Approach Flow," in *2018 AIAA Aerospace Sciences*, Kissimmee, Florida, 2018.

[7] M. Albrecht, A. M. Naguib M. M. Koochesfahani, "A Study of the Aerodynamics of a Low Reynolds Number Airfoil Translating Across a Uniform-Shear Approach Flow," in *AIAA SciTech*, San Diego, California, 2019.

[8] D. R. Kotansky, "The Use of Honeycomb for Shear Flow Generation," *AIAA Journal*, vol. 4, no. 8, pp. 1490-1491, 1966.

[9] A. Safaripour, D. Olson, A. M. Naguib M. M. Koochesfahani, "On Using Shaped Honeycombs for Experimental Generation of Arbitrary Velocity Profiles in Test Facilities," *Bulletin of American Physical Society*, vol. 61, p. 265, 2016.